Bleomycin Induces Fibrotic Transformation of Bone Marrow Stromal Cells to Treat Height Loss of Intervertebral Disc Through the TGFβR1/Smad2/3 Pathway

Xiao Yang
Shanghai 9th Peoples Hospital Affiliated to Shanghai Jiaotong University School of Medicine
zhiqian chen
Shanghai 9th Peoples Hospital Affiliated to Shanghai Jiaotong University School of Medicine
Chen Chen
Shanghai 9th Peoples Hospital Affiliated to Shanghai Jiaotong University School of Medicine
Chen Han
Shanghai 9th Peoples Hospital Affiliated to Shanghai Jiaotong University School of Medicine
Yifan Zhou
Shanghai 9th Peoples Hospital Affiliated to Shanghai Jiaotong University School of Medicine
Xunlin Li
Shanghai 9th Peoples Hospital Affiliated to Shanghai Jiaotong University School of Medicine
Haijun Tian
shanghai 9th
Xiaofei Cheng
Shanghai 9th Peoples Hospital Affiliated to Shanghai Jiaotong University School of Medicine
Kai Zhang
Shanghai 9th Peoples Hospital Affiliated to Shanghai Jiaotong University School of Medicine
An Qin
Shanghai 9th Peoples Hospital Affiliated to Shanghai Jiaotong University School of Medicine
Tangjun Zhou
Shanghai 9th Peoples Hospital Affiliated to Shanghai Jiaotong University School of Medicine
Jie Zhao (✉ profzhaojie@126.com)
Shanghai Jiao Tong University School of Medicine https://orcid.org/0000-0003-1000-5641

Research

Keywords: Intervertebral Disc Degeneration, Bleomycin, Bone Marrow Stromal Cells, Annulus Fibrosus Cells, Reparative Fibrosis, TGFβ-TGFβR1-SMAD2/3 Signaling Pathway

Posted Date: September 4th, 2020

DOI: https://doi.org/10.21203/rs.3.rs-71602/v1

Version of Record: A version of this preprint was published on January 7th, 2021. See the published version at https://doi.org/10.1186/s13287-020-02093-9.

Abstract

Background: Lower back pain is often accredited to loss of intervertebral disc (IVD) height and compromised spine stability as a result of intervertebral disc degeneration (IVDD). We aim to locally use Bleomycin to induce the fibrotic transformation of bone marrow stromal cells (BMSCs) as a means to induce reparative fibrosis to slow down the height loss.

Methods: IVD from patients were gathered for histological examination. The expression of transforming growth factor beta 1 (TGF-β) signaling pathway was determined by qPCR and western blotting. Nucleus pulposus (NP) cells, annulus fibrosus (AF) cells and the Rats' bone marrow stromal cells (BMSC)were cultured and their responsiveness to Bleomycin was evaluated by Cell Counting Kit-8, comet assay, transwell migration and wound healing assays. Rat IVDD models were created by puncture, rescued by Bleomycin injection and the effectiveness was evaluated by images (X-ray and MRI) and atomic force microscope.

Results: Histological examination showed increased levels of pro-fibrotic markers in IVDD tissues from patients. AF cells and BMSC cells was induced to adopt to a pro-fibrotic phenotype with increased expression fibrotic markers Col1a1, Col3a1, FSP1. The pro-fibrotic effect of Bleomycin on AF cells and BMSCs was in part due to the activation of the TGFβ-TGFβR1-SMAD2/3 signaling pathway. Pharmacological inhibition or gene knock-down of TGFβR1 could mitigate the pro-fibrotic effects.

Conclusion: Locally injection of Bleomycin in rats' IVD induced rapid fibrosis and maintained its height through TGFβ-TGFβR1-SMAD2/3 signaling pathway.

Background

Low back pain and other spine disorders due to intervertebral disc degeneration affects over 600 million of people worldwide, imposing substantial burden to the medical and socioeconomic structures of all developed countries[1]. Intervertebral disc degeneration is a complicated process involving three main tissues: the nucleus pulposus (NP), a proteoglycan-rich gelatinous center of the intervertebral disc; the outer and inner anulus fibrosus (AF), a partially concentric collagen-rich fibrocartilaginous tissue surrounding the NP; and two cartilaginous endplates that interface with the vertebral bodies superiorly and inferiorly[2-4] . Intervertebral disc degeneration is a progressive, cell-mediated cascade of molecular, structural and biomechanical changes: degeneration starts in the NP where the reduction in proteoglycan content and a decrease in the ratio of proteoglycan to collagen results in loss of hydrostatic properties leading to structural wear and compromised biomechanical functions[5]. Continued dehydration results in the collapse of the NP, loss of intervertebral disc height and the gradual loss of NP-AF borders ultimately progressing to complete degeneration of the entire intervertebral disc. This causes spine instability and nerve root compression evoking chronic back pain[5, 6].

During degeneration in discs, ruptured NP and AF would recruit multiple cells to finish the repair process, of which the most important cells are fibroblastic cells and MSCs[7], but due to the low cell population

and lack of nutrient supply to the intervertebral disc tissues, self-regeneration is limited[6, 8, 9]. Conventional treatment strategies are largely limited to symptomatic relief with limited long-term efficacy[10-12], and this spinal fusion surgery does no restore biomechanical properties but may in fact induce degeneration of adjacent vertebral bodies due to the increased mechanical stress they have to sustain[13-15]. Cell-based approach has also been studied in the past few years and one of the most focused methods is disc regeneration via MSCs transplantation[16-18]. Moreover, recent researches have unveiled that there are some MSCs distributed around the outer AF region and endplate[19]. So from a different perspective that a former approach of our studies by injection of autologous dermal fibroblast cells into degenerative intervertebral to treat IVDD[20]: We showed that the induction of reparative fibrosis combined with two essential cells in discs, one is to induce the fibrotic phenotype of MSCs, and the other is to promote the fibroblastic-like cell AF cells.

Bleomycin is a cytotoxic chemotherapeutic compound used in the treatment of lymphoma, leukemia, squamous cell carcinomas, and some genital tract tumors. Its major side-effect as an anti-cancer agent is the induction of fibrosis particularly pulmonary fibrosis. Because of this effect, Bleomycin has been used as the ‘gold-standard’ agent to induce experimental pulmonary fibrosis in various animal models. To avoid the side effects of system-used Bleomycin, Lin X et al used intralesional interstitial Bleomycin injection to treat extracranial arteriovenous malformation. This prospective study involved 34 patients and finally successfully cure 27 of them making an extraordinary result with less side effects[21, 22]. Based on these studies, we hypothesized that the pro-fibrotic effects of Bleomycin using locally injection could be exploited to induce fibrosis in degenerative intervertebral discs.

In this study, we investigated the potential use of Bleomycin to induce reparative fibrosis as a means to maintain intervertebral disc height, and we tried to use it to induce the fibrosis phenotype of BMSCs and offer an alternative treatment in degeneration caused height loss. We also explored the potential molecular mechanism underlying the effects Bleomycin particularly in terms of the TGFβ-SMAD2/3 signaling, a key pathway in the fibrotic process.

Methods

Intervertebral discs specimens

Intervertebral discs (≥ 5 mm) were obtained from 12 patients, including 7 males and 5 females with a combined average age of 52.8 ± 12.8 years (age range of 30-74 years) and diagnosed with lumbar disc herniation (LDH) or degenerative lumbar spondylolisthesis (DLS) (Figure 1A – C; Table 1). The NP were sampled from L4/5 and subjected to histological and immunohistochemical analyses. Intervertebral disc degeneration was evaluated using the Pfirrmann grading system.

Isolation and cell culture of BMSCs

6-week-old male Sprague-Dawley rats (Shanghai Lab, Animal Research Center Co. Ltd, Shanghai, China) were killed by cervical dislocation and soaked in the 75% ethanol for 10 min. Extraction and isolation of

BMSCs from two lower legs of SD rats with sterile operation, BMSCs were cultured in Minimum Essential Medium α (MEMα) supplemented with 10% FBS and 1% penicillin-streptomycin (Gibco, Thermo Fisher Scientific, Waltham, MA, USA).

Culture of NP and AF cell-lines

The Rat's NP and AF cell are immortalized cell lines[23] which were kindly gifted by Dr. Chen Di at the Department of Orthopedic Surgery, Rush University Medical Center (Chicago, IL, USA). Cells were maintained in Dulbecco's modified Eagle's medium (DMEM) supplemented with 10% FBS and 1% penicillin-streptomycin (Gibco, Thermo Fisher Scientific, Waltham, MA, USA).

RNA extraction and real-time quantitative PCR (qPCR) analyses

Total RNA were isolated from tissues and cells using TRIzol reagent (Thermo Fisher Scientific, Waltham, MA, USA) as per manufacturer's protocol. First strand complementary DNAs (cDNAs) were reversed transcribed from extracted RNAs using the cDNA Synthesis Kit (Takara Bio, Otsu, Japan). Relative mRNA expression was determined by RT-PCR using the GoTaq 1-step RT-qPCR System (Promega, Madison, WI, USA) followed by agarose gel electrophoresis (Bio-Rad Laboratories, Hercules, CA, U.S.A). Real-time qPCR was conducted using the TB Green Premix Ex Taq Kit (Takara Bio) on an Applied Biosystems QuantStudio 6 Flex Real-Time PCR System (Thermo Fisher Scientific). Specific primer pairs were designed using NCBI BLAST and sequences provided in Table 2. The gene expression of GAPDH or β-actin was used as internal control. Target gene expression levels were determined using the $2^{-\Delta\Delta CT}$ method. The mean CT value of target genes in the experimental groups were normalized to the CT value of GAPDH or β-actin to give a ΔCT value. This was then further normalized to control samples to obtain ΔΔCT.

Cell viability analysis

Cell viability following Bleomycin treatment was evaluated using the Cell Counting Kit-8 (CCK-8; Dojindo Laboratories Co., Ltd, Kumamoto, Japan). Cells seeded onto 96-well plates at a density of 8×10^3 cells/well the day before were treated with increasing concentrations of Bleomycin sulfate (1, 5 and 10 μg/ml, dissolved in PBS; Selleck Chemicals, Houston, TX, USA) for 24, 48, 72, and 96 hours. NP, AF and BMSC cells were cultured in DMEM, DMEM/F12 or MEMα respectively, all supplemented with 10% FBS and 1% penicillin/streptomycin (complete DMEM or complete DMEM/F12). Cell media containing Bleomycin were changed every 2 days. At the end of the experimental periods, cells were incubated with fresh complete media containing 10 μl of CCK-8 reagent for 1 hour at 37°C. Complete media containing CCK-8 reagent but no cells and untreated cells were used as a blank and mock controls respectively. The absorbances (measured as optical density; OD) at 450 nm were measured on an Infinite M200 Pro multimode microplate reader (Tecan Life Sciences, Männedorf, Switzerland). ODs of the Bleomycin treated groups were normalized to corresponding blank ODs to account for background interference.

TGFβR1 siRNA knockdown

AF cells seeded onto 6-well plates at a density of 1×10^5 cells/well the day before were tranfected with small interfering RNA (siRNA) against TGFβR1 (siTGFβR1: Sense 5′- GGAGAUUGUUGGUACCCAAGG-3′; and Anti-sense 5′-UUGGGUACCAACAAUCUCCAU-3′) or with a scrambled siRNA control (NC: Sense 5′-UUCUCCGAACGUGUCACGUTT-3′; and Anti-sense 5′-ACGUGACACGUUCGGAGAATT-3′) (IBSBIO, Shanghai, China) using Lipofectamine 3000 transfection reagent in accordance with manufacturer's protocol. After 6 hours, media containing transfection reagent and siRNAs were removed and replaced with fresh complete media. Twenty-four hours post-transfection cells were harvested for total protein or total RNA extraction.

Comet analysis (single cell gel electrophoresis)

The method for comet analysis or single cell gel electrophoresis (SCGE) was performed as previously described[24, 25] Briefly, cultured AF and NP cells were trypsinized, centrifuged and resuspended in 1×PBS (Ca^{2+} and Mg^{2+} free; Gibco, Thermo Fisher Scientific) to final cell density of 1×10^5 cells/ml. Next, 50 µl of cell suspensions were then mixed with 500 µl low melting point (LMP) agarose (1% at 37°C, Comet SCGE Assay Kit; Enzo Life Sciences, Farmingdale, NY, USA) and then 75 µl of cell-agarose mixture were spread onto glass slides precoated with 1% normal melting point (NMP) agarose and allowed to settle for 10 mins at 4°C in the dark. Slides were then immersed in pre-chilled Lysis Solution (Comet SCGE Assay Kit; Enzo Life Sciences) and incubated on ice for 1 hour. After lysis, the slides were placed on a horizontal gel electrophoresis unit containing electrophoretic Alkaline Solution (Comet SCGE Assay Kit; Enzo Life Sciences) for 60 mins at room temperature in the dark to allow the DNA to unwind. Electrophoresis was then carried out for 10 mins at 25 V and 300 mA (0.73 V/cm). After electrophoresis, slides were rinsed in distilled water, placed in neutralization solution (pH 7.5) to remove alkali and detergent, then dehydrated with 70% ethanol for 5 minutes and air-dried. Immediately before examination, the slides were stained with 100 µl of ethidium bromide (10 µg/ml) for 30 mins at room temperature in the dark. Comets were visualized under 400× magnification using epifluorescence microscopy (Leica DM4000 B; Leica Microsystems, Wetzlar, Germany)

Scratch-wound healing assay

The scratch-wound healing assay was performed to examine the effects of Bleomycin on collective migration and recolonization in a 2-dimensional environment. AF cells with or without TGFβR1 siRNA knockdown and BMSCs were cultured to 100% confluence. Under sterile conditions, a linear scratch line was made straight down the centre of the cell monolayer using the tip of a sterilized 200 µl micropipette tip. Cell media were carefully aspirated to remove cellular debri and floating cells and then replaced with fresh serum-free DMEM/F12 or MEMα without or with Bleomycin (5 or 10 µg/ml) ± TGFβR1 inhibitor (LY364947, 10µM; Selleck, USA). Phase contrast images were captured of the initial scratch wound for reference and designated time 0. Further images were captured at 24 and 48 hours, and the distance between the leading cell edges at each time point was measured using Imagej software (National Institutes of Health, USA).

Millicelltranswell migration assay

The effects of Bleomycin on single cell migration through three-dimensional environment were examined using the transwell migration assay (Millicell Standing Cell Culture Inserts, 8 μm pore size; Merck-Millipore, Burlington, MA, USA). Briefly, AF cells with or without TGFβR1 siRNA knockdown and BMSCs were seeded into the upper chamber of the Millicell Standing Cell Culture inserts at a density of 8×10^4 cells/well in serum-free DMEM/F12 or MEMα media without or with Bleomycin (5 or 10 μg/ml) ± TGFβR1 inhibitor (LY364947, 10μM; Selleck, USA). The inserts were then placed into 24-well plates filled with complete media (FBS as chemoattractant source) and cultured for 24 hours. At the end of the experiment, media in the inserts were discarded and adherent cells were fixed in 4% paraformaldehyde (PFA) for 30 mins and then stained with 0.2% crystal violet for 5 mins. Cells adhering to the membrane inside the inserts (i.e. cells that have not migrated) were gently removed using a cotton-tipped applicator. Migrated cells on the other side of the inserts were imaged under a light microscope (Leica DM4000 B; Leica Microsystems) and staining intensity analyzed with Image Pro Plus 6.0 software to evaluate the ratio of integrated optical density (expressed as the IOD/area for each sample).

Assessment of apoptosis by flow cytometry

The effects of Bleomycin on cell apoptosis was evaluated using flow cytometry following staining with APC-Annexin V and propidium iodide (PI) based apoptosis staining kit (Thermo Fisher Scientific) according to manufacturer's protocol. Briefly, AF and NP cells seeded in 6-well plates at a density of 2×10^5 cells/well were treated with 5 or 10 μg/ml Bleomycin for 72 hours, after which cells were then harvested by trypsinization and centrifugation. Cell pellets were gently resuspended in 1× binding buffer containing APC-Annexin V and/or PI reagent and incubated at room temperature for 15 mins in the dark. Cell suspensions were subjected to flow cytometry on a FACSCalibur Flow Cytometer (BD Biosciences) counting at least 10000 events. The apoptotic rate was quantified based on the percentage of cells in the right upper (Q2; positive staining for APC-Annexin V and PI) and right lower (Q3; positive staining for APC-Annexin V and negative for PI) quadrant of the flow cytometric scatterplot.

Western blot analysis

Total cellular proteins were extracted from cultured cells using RIPA lysis buffer supplemented with phosphatase and protease inhibitors (Roche, Basel, Switzerland). Equal quantities of extracted proteins (20-30 μg) were resolved on 10% or 12.5% SDS-PAGE gel and separated proteins electroblotted onto 0.22 μm PVDF membranes (Merck-Millipore). Membranes were blocked with 5% BSA-PBS at room temperature for 1 hour and then incubated with primary antibodies (diluted 1:1000 in 5% BSA-PBS) overnight (at least 16 hours) at 4°C. Primary antibodies against SMAD2 (Ser308, D43B4; rabbit mAb), phospho-SMAD2 (Ser465/467, 138D4; rabbit mAb), SMAD3 (C67H9; rabbit mAb), phospho-SMAD3 (Ser423/425, C25A9; rabbit mAb), SMAD2/3 (D7G7; rabbit mAb), phosphor-SMAD2/3 (Ser465/467; Ser423/425; rabbit mAb), SMAD4 (D3M6U; rabbit mAb) and β-actin (D6A8; rabbit mAb) were purchased from Cell Signaling Technology (Danvers, MA, USA). Primary antibodies against FSP1(S100A4; rabbit mAb), TGFβ Receptor I

(ab31013; rabbit mAb), type I collagen (ab6308; rabbit mAb), and TGFβ1 (ab64715; rabbit mAb) were obtained from Abcam (Cambridge, UK). Membranes were then washed extensively in Tris-buffered saline-Tween20 (TBST) and subsequently incubated with anti-rabbit IgG (H+L) (DyLight™ 800 4× PEG Conjugate; Cell Signaling Technology) secondary antibody (1:5000 dilution) for 1 hour at room temperature in the dark. Membranes were again extensively washed in TBST and protein immunoreactivity were detected on a LI-COR Odyssey Fluorescence Imaging System (LI-COR Biosciences, Lincoln, NE, USA). Semi-quantitative analysis of protein immunoreactive band intensity were measured using Image-Pro Plus 6.0 software and normalized to the internal loading control β-actin.

Animals and surgical procedures

All animal experimentation were approved by the Institutional Animal Care and Ethics Committee of Ninth People's Hospital, Shanghai Jiaotong University School of Medicine (Shanghai, China) and performed in accordance with the principles and procedures of the National Institutes of Health (NIH) Guide for the Care and Use of Laboratory Animals and the Guidelines for Animal Treatment of Shanghai Jiaotong University. Six 8-week-old male Sprague-Dawley rats (Shanghai Lab, Animal Research Center Co. Ltd, Shanghai, China) were housed under pathogen-free conditions at 26-28°C and 50-65% humidity with 12-hour day/night cycle. Animals were fed standard rodent chow and had access to fresh water *ad libitum*. Before surgical procedures, rats were anesthetized by intraperitoneal injections of pentobarbital sodium (5 mg/100 g of body weight). The tails were sterilized with iodinated polyvinylpyrrolidone and then a ventral longitudinal skin incision was made over the tail to reveal the intervertebral disc at coccyx vertebrae 6-10. The intervertebral discs at Co6/7 were used as Sham controls and the intervertebral discs at Co7/8, Co8/9 and Co9/10 were used as experimental groups. Intervertebral discs were punctured with a 20-gauge sterile needle oriented perpendicular to the skin to make ensure insertion at the center of the disc level through the AF into the NP. The incision was then sutured and rats were allowed post-operative recovery for two weeks. A group of mice (n = 3) were sacrificed and the tails extracted, cleaned of soft tissues and the vertebral column fixed in 4% PFA. To the remaining rats (n = 3), surgical exposure of the intervertebral discs at Co8/9 and Co9/10 was again carried out, and 5μl of Bleomycin at concentrations of 10 and 5 μg/ml was injected respectively into each disc. Incision was sutured and rats were allowed 2 and 4 weeks of post-treatment recovery. At the end of the experimental period, all remaining rats were sacrificed and the tails extracted, cleaned of soft tissues and the vertebral column fixed in 4% PFA.

Histology and immunofluorescence staining

Fixed intervertebral disc tissue samples were embedded into paraffin blocks then subjected to histological sectioning (5 μm thickness). For histological assessment, paraffin tissue sections were processed for Safranin O-Fast Green and Sirius Red staining in accordance with standard laboratory protocols. For immunofluorescence assessment, BMSCs were cultured in a slide with a confluence of 10% and fixed with 4%PFA, then these cell slides are with tissue sections to be de-paraffinized in graded xylene, rehydrated in graded alcohol solutions and then incubated in antigen retrieval buffer (Roche) at 37°C for 30 mins. After cooling to room temperature, slides were immersed in PBS (pH 7.4) and washed 3

times for 5 mins each. Auto-fluorescence quencher was added to the sections for 5 mins, and then blocked with blocking buffer for 30 mins at room temperature. Sections were subsquently incubated with primary antibodies in a wet box at 4°C overnight. Primary antibodies were used at 1:100 dilution and included anti-Col1a1, anti-Col2a1, anti-FSP1, anti-TGFβ, and anti-TGFβR1 (all purchased from Cell Signaling Technology). The next day, sections were washed with PBS and then incubated with Alexa Fluor 594 Conjugate secondary antibody (anti-rabbit, 1:500; Cell Signaling Technology) for 50 mins at room temperature in the dark. Sections were washed with PBS and then incubated with DAPI solution (Sigma-Aldrich, St Louis, MO, USA) for 10 mins in the dark to stain cell nuclei. Sections were subjected to final PBS washes, air-dried and then sealed with anti-fluorescence quenching tablets. Digital fluorescence images were captured under a Leica DM4000 B epifluorescence microscope (Leica Microsystems) and IOD measurements carried out using Image Pro Plus 6.0 software.

Radiographic and magnetic resonance imaging (MRI) analysis

Digital X-ray imaging of the punctured intervertebral discs were conducted in the anteroposterior axis with a 21 lp/mm detector that provides up to 5× geometric magnification (Faxitron VersaVision; Faxitron Bioptics LLC, Tucson, AZ. USA). MRI imaging of the same punctured intervertebral discs were carried out on a Siemens Magnetom Prisma E11 (Siemens Healthineers, Erlangen, Germany) with the following parameters: TR 3000 ms, TE 80 ms, 1.1 mm thickness, 0.22 mm interval, FOV 160×65 mm, and voxel size 0.25×0.25×1.1 mm.

Atomic Force Microscopy (AFM)

For AFM, the extracted punctured vertebrae were dissected to make paraffin section and nanoindentation was performed on a Park NX20 (Park Systems, South Korea) equipped with microspherical colloidal tips (R < 10 nm, nominal $k \approx 0.2$ N/m, Tip:Si/Tipless/Top, cantilever Si/Al/Top; Park Systems). For a wide range of undulating surfaces, the scanning rate of 13 Hz was used. Large scanning rate can reduce drift, but it is generally only used for scanning small flat surfaces. Indentation was applied at a z-piezo displacement rate of 10 μm/s to a maximum load of ~120 nN using a Scan Asyst-Air probe, a curvature radius of 5 nm, and a force constant of 0.4 N/m. Young's modulus, adhesion force, deformation parameters were evaluated.

Statistical analysis

Three independent experiments or repeated measurements were conducted for all data. Data are presented as the mean ± standard deviation (S.D.). Significance differences between study groups were obtained by Student's *t*-test or one-way analysis of variance (ANOVA) using SPSS 19.0 software (IBM Corporation, Armonk, NY, USA). Statistical significance was set at a *If the p*-value < 0.05 unless otherwise indicated.

Results

Intervertebral disc degeneration correlates with fibrotic changes in NP in patients with lumbar disc herniation or degenerative lumbar spondylolisthesis.

Degenerative and fibrotic changes in the intervertebral discs from 12 patients (patient details presented in Table 1) with lumbar disc herniation (LDH) or degenerative lumbar spondylolisthesis (DLS) were examined by MRI and Safranin O-Fast Green (SOFG) histological staining (Figure 1A-C). Pfirrmann grading based on MRI scans[6, 10]were then correlated with degree of fibrosis based on IOD of SOFG staining in the NP tissues of the intervertebral disc (Figure 1D). Consistent with the Pfirrmann grading for intervertebral disc degeneration, the higher the Pfirrmann grade, the greater the degree of the NP fibrosis in the intervertebral discs as demonstrated by increasing IOD score of Fast Green staining in the tissue sections (Figure 1D). That is, higher Pfirrmann grade is correlated with greater fibrotic changes in the NP tissues. We further noticed that with higher Pfirrmann grade such as IV and V (severe intervertebral disc degeneration with or without collapsed disc space), the fibrotic changes occurs closer to the center of the NP tissues in the intervertebral disc (Figure 1B-D). No fibrosis was seen in intervertebral discs that were presented as Pfirrmann grade III (Figure 1A and D). We also examined the expression of fibrotic protein markers between the non-fibrotic and fibrotic regions of the NP tissues (Figure 1E and F). Compared with the non-fibrotic region, the fibrotic region expressed high levels of protein markers involved in fibrosis such as Col1a1, FSP1, TGFβ, and TGFβR1, and markedly decreased levels of Col2a1 (Figure 1E and F). Of these markers, FSP1 or fibroblast-specific protein-1 is highly expressed in fibroblasts and often used as fibrotic biomarker. The elevated expression of TGFβ and TGFβR1 suggests involvement of TGFβ signaling pathway in inducing fibrotic changes in the NP region during intervertebral disc degeneration.

BMSCs was induced to acquire fibrotic phenotype by Bleomycin *in vitro*

Our previous research using a cell-based approach have shown that induction of reparative fibrosis may offer beneficial effects against the progression of disc degeneration[20], and this process is associated with TGFβ signaling pathway. Considering the Bleomycin is an effective trigger to induce the upregulation of TGFβ in lung epithelium cells[26] and have been used in clinical situation before , we tried to use bleomycin combined with the multipotentiality of BMCSs to induce their fibrotic differentiation. In our research, Bleomycin could efficiently promote the migration of BMSCs in wound healing assay and transwell test (Figure 2A and 2B). Then, we showed that the cell viability of BMSCs were minimally deteriorated by the bleomycin in a concentration of 5 and 10ug/ml with a duration of 24 hours and 72 hours (Figure 2C).This enhancement in the ability of migration may be the consequence of changes happened in the molecular level, including the upregulation of TGFβR1 and TGFβ gene, as well as the expression of pro-fibrotic marker genes Col1a1, FSP1 and Fn1(Figure 2F). Moreover, in the western blotting test we detected the slight elevation of TGFβR1, Col1a1, FSP1 with the stimulation of Bleomycin (Figure 2D). Immunofluorescence staining was carried out and we got the same result that TGFβ and Col1a1 increased with the Bleomycin (Figure 2E). To further confirmed our hypothesis, we use LY363947 (10μM)[27], a TGFβR1 kinase activity inhibitor, to treat BMSC cells with Bleomycin and found that it markedly inhibited AF cell migration in both the scratch-wound healing and the transwell migration assay

(Figure 2A and 2B), and it also could mitigate the upregulation of these pro-fibrotic marker genes and proteins mentioned above (Figure 2E and 2F).

Bleomycin shows little cytotoxicity in AF cells *in vitro*

Bleomycin is a chemotherapeutic cytotoxic compound that inhibits DNA metabolism and causes free-radical based DNA damage, So here we assessed the effects of Bleomycin in the intervertebral disc. We first examined the cellular effects of Bleomycin on cells of the intervertebral discs particularly AF and NP cells. As shown in Figure 3A and B, Bleomycin exerted little cytotoxic effects on AF and NP cells following 24 hours treatment. For AF cells a trend of decrease in cell viability was observed at all doses of Bleomycin when cells were treated for 48 and 72 hours, but the cytotoxic effect was only statistically significant in 96 hours (Figure 3A). On the other hand, significant reduction in cell viability was observed in NP cells treated with 10 µg/ml of Bleomycin for 48, 72, and 96 hours, and with 5 µg/ml of Bleomycin at 96 hours. (Figure 3B). Next we employed flow cytometry to examine whether the cytotoxic effects of Bleomycin on NP cell viability was due to the induction of apoptosis. As shown in Figure 3C, a greater percentage of NP cells underwent cell death (necrotic and apoptotic) following 72 hours of Bleomycin treatment (at both 5 and 10 µg/ml) when compared with untreated controls as well as with AF cells. Both early (LR; lower right quandrant) and late (UR; upper right quandrant) apoptotic rate in NP cells were significantly and dose-dependently (Figure 3D and 3E). Similar effect was seen for cell necrosis (Suppl. Figure 1A). On the other hand, the percentage of cells that underwent necrosis (Suppl. Figure 1A), early apoptosis (Figure 3D), and late apoptosis (Figure 3E) in AF cells following Bleomycin treatment were similar to untreated controls. Consistent with elevated apoptotic tendencies, NP cells treated with Bleomycin was found to exhibit reduced expression of Cyclin D1, a cell cycle regulatory protein, and concomitant increase in the levels of cleaved Caspase 3, a crucial executor caspase in the apoptotic signaling cascade (Suppl. Figure 1B).In cells' level, single cell gel electrophoresis or comet analysis was carried out. Figure 3F and G showed that Bleomycin dose-dependently induces significant DNA strand breaks and formation of markedly long comet tails in NP cells, evidenced by fluorescence intensity of DNA in the head and tail of the comet. Although DNA breaks and comet tails were also observed in Bleomycin treated AF cells (Figure 3F), the degree of DNA damage was significantly less than in NP cells both in a dose- and time-dependent manner (Figure 3G). Taken together, our results show that NP cells are more susceptible to the cytotoxic and DNA damaging effects of Bleomycin than AF cells.

Bleomycin promotes AF cell migration *in vitro* via TGFβ-TGFβR1 signaling.

Considering the AF cells are fibroblast-like cells and the TGFβ signaling pathway functioned in the fibroblast cells' migration[28]. We detected the collective migratory behavior of AF cells using the *in vitro* scratch-wound healing assay. When compared to untreated controls, Bleomycin treatment dose-dependently enhanced AF cell migration and scratch-wound closure at 24 and 48 hours after the creation of the scratch wound creation (Figure 4A and Suppl. Figure 2A). To better mimic the *in vivo* behavior of individual AF cells, the transwell directional migration assay was performed. As shown in Figure 4C, AF cells that migrated through the transwell inserts were stained with crystal violet. Furthermore, consistent

with the scratch-wound healing migration assay, Bleomycin treatment significantly increased the number of AF cells that migrated through the transwell insert (Suppl. Figure 2B). This suggests that activated TGFβ-TGFβR1 signaling is involved in mediating the effects of Bleomycin on AF cells. To further confirm that this was the case, TGFβR1 gene silencing in AF cells was carried out followed by Bleomycin treatment and migration assays. Consistent with the inhibitory effects of LY363947, the knockdown of TGFβR1 significantly attenuated Bleomycin-induced AF cell migration in both the scratch-wound healing and transwell migration assays (Figure 4B and D; and Suppl. Figure 2C and D).

Bleomycin activates the TGFβ-TGFβR1-SMAD2/3 signaling pathway in AF cells

To further decipher the molecular mechanism for the effects of Bleomycin on AF cells, biochemical analyses of gene and protein expression were carried out. As shown in Figure 5H and Suppl. Figure 3A, Bleomycin treatment induced the upregulation TGFβR1, TGFβR2 and TGFβ gene expression, as well as the expression of pro-fibrotic marker genes Col1a1, Col3a1 and Fn1, but no change in TGFβR3 gene expressions were observed. Pharmacological treatment with LY363947 inhibited Bleomycin-induced upregulation of TGFβR1, Col1a1, Col3a1 and Fn1 gene expression, but had little effect on TGFβ and TGFβR2. Silencing of TGFβR1, of which the knock-down efficiency is approximately 66.9%, significantly inhibited these changes better than LY363947 treatment but still couldn't inhibited TGFβ and TGFβR2 neither (Figure5H and Suppl. Figure 3B). None-the-less, these results indicate that Bleomycin induced AF cells to adopt a stronger fibrotic phenotype.

Immunoblot analyses were then carried out to examine the activation state of TGFβ-TGFβR1 signaling following Bleomycin treatment. In our immunoblot assays, we showed that Bleomycin treatment induced the expression of TGFβ and TGFβR1(Figure 5E), and the fibroblast marker FSP1 and profibrotic protein Col1a1 was similarly induced. On the other hand, silencing of TGFβR1 abolished the Bleomycin-induced protein expression of Col1a1 and FSP1 (Figure 5E). Furthermore, considering the downstream activation of SMAD2/3 transcription factors are important drivers of fibrosis, phosphorylation of SMAD2 and SMAD3 were analyzed a following Bleomycin treatment (Figure 5A and 5B). However, pre-treatment of AF cells with LY363947 abolished the Bleomycin-induced activation of TGFβ-TGFβR1-SMAD2/3 signaling (Figure 5C and 5D). Similar inhibitory effects against Bleomycin-induced activation of TGFβ-TGFβR1-SMAD2/3 signaling was seen following TGFβR1 gene silencing (Figure 5F and 5G).

Bleomycin induces fibrosis in degenerative intervertebral discs and maintains disc height *in vivo*.

Using a needle puncture model of intervertebral disc degeneration in rats, we validated the potential use of Bleomycin to induce reparative fibrosis for the maintenance of disc height. Disc degeneration was allowed to develop for 2 weeks after needle puncture prior to administration of Bleomycin therapy for further 2 and 4 weeks (Suppl. Figure 3C, E and F). X-ray and MRI imaging were carried out to evaluate the effects of Bleomycin therapy (Figure 6A and 6B). X-ray radiographs show that the intervertebral dics that underwent needle puncture without subsequent Bleomycin treatment (Co7/8) showed progressive disc degeneration including height loss and disc collapse by the end of the experimental procedure (Figure 6A). MRI scans further show disc degeneration with progressive increase in grey levels (loss of T2 signal

intensity) in the needle puncture only intervertebral discs (Figure 6B). In contrast, intervertebral discs that received Bleomycin therapy (Co8/9, 10 μg/ml; and Co9/10, 5 μg/ml) exhibit little degenerative features and maintenance of disc height despite the progressive loss of T2 signal intensity (Figure 6A and 6B). No degeneration of the intervertebral discs was observed in the sham group.

Histological examinations were then carried out to further assess the microstructural changes following Bleomycin therapy (Figure 6C and 6D). In both SOFG and Sirius Red stained intervertebral disc sections, AF and NP boundaries are clearly demarcated with no signs of disc degeneration (Figure 5C). Lack of collagen content was observed in the NP, whereas AF exhibits abundant type 3 and type 1 collagen (Figure 6C and 6D). Following needle puncture, we can see the loss of disc heigh and collapse of the intervertebral discs, increased type 3 collagen content in the NP indicating the onset of fibrosis (Figure 6C and 6D). However, no fibrosis into the remaining NP was observed (Figure 6C). In stark contrast, the boundaries between the AF and NP were not discernible in the Bleomycin therapy groups, with the NP completely filled with concentric lamellar type I collagen 1 (Figure 6C and 6D). However, the formation of such fibrous tissue resulted in the maintenance of the intervertebral disc height (Figure 6C). Immunofluorescence staining was further carried out to assess the expression of pro-fibrotic markers in the intervertebral discs. As shown in Figure 6E, untreated degenerative discs exhibited slightly elevated expression of TGFβ, TGFβR1, Col1a1 and FSP in the NP when compared to sham controls. Consistent with *in vitro* effects, Bleomycin administration significantly upregulated the expression of TGFβ, TGFβR1, Col1a1 and FSP in the AF and NP.

Atomic force microscopy (AFM) was subsequently carried out to evaluate the structural properties and stress tolerance, which was described by the Young's modulus (a measure of ability to withstand elastic/recoverable deformation under lengthwise tension or compression; a measure of stiffness), adhesion force, deformation and the topography correlated with the displacement curve(Suppl. Figure 4B and 4D). With puncture the Young's modulus increased in AF region, but after Bleomycin injection, the Young's modulus was even significantly higher (Figure 5F and 6G). Conversely, we observed elevation of the Young modulus in the NP region while puncture, but there was relative recovery after Bleomycin rescue (Suppl. Figure 4A and 4C), meaning the NP region could maintain the nature biomechanical status with bleomycin. Collectively, these results provide evidence that Bleomycin therapy can accelerate the IVD fibrosis and strengthen the discs' anti-stress ability without loss of the disc height.

Discussion

The incidence of intervertebral disc degeneration is increasing in an alarming rate in our modern society, and the height loss happened during degeneration is the major cause of neurological symptoms. Following with the height loss was the change of biomechanical characteristic[29] and the possible compression of nerve root in intervertebral foramina[30, 31], so aiming at maintaining even restoring the height is the effective treatment to solve the problem. However, a lack of effective early and mid-term treatment options to maintain the height is available with most end-stage disease treated surgically via discectomy and interbody spinal fusion. Some previous research tried to use the regeneration methods to

maintain the disc height, like A bio-scaffold composed of decellularized nucleus pulposus and native nucleus pulposus[32] or just a in situ gelling alginate hydrogel[33] alone, and in our research we offered a new hypothesis that the reparative fibrosis model combined BMSCs and Bleomycin might be an alternative choice to treat IVDD.

Disc fibrosis is in fact a compensatory process during disc degeneration, but the cells functioned during this process still has been debated during the past few years. Some researchers have found that there are some proliferated cells which shared same markers with MSCs in the human degenerated IVDs [34, 35], these cells are distributed mainly in the endplate or outer AF region[36] and their migration rate and endogenous repair mechanism still need to be determined[19, 37]. From our previous observations in patients, we observed fibrotic changes in the acute phase of lumbar disc herniation as well as fibrosis of the intervertebral disc after percutaneous endoscopic lumbar discectomy. Such changes could represent an initial compensatory protective mechanism to maintain the height of the intervertebral disc and spine, which the MSCs may play an important and initial role during this process. Hence from our perspective, we advocate to activate the MSCs and fibroblast-like cells, promote its ability of migration and collagen deposition aiming at finally alternate the declining NP tissues and successfully maintain even restore the disc height .The induction of reparative and fast fibrosis in degenerative intervertebral discs could offer a way for tissue repair and spine stabilization. We and others have previously shown that reparative fibrosis define here as the formation of organized scar tissue necessary to mechanically stabilize the degenerative intervertebral disc, have potential beneficial effects against the height loss during intervertebral disc degeneration[20, 38]. The use of dermal fibroblast-based cell therapy was found to induce degenerative intervertebral disc fibrosis, prevent the loss of disc height and disc collapse, and maintain the biomechanical properties of the spine[39, 40].

In this study, we use Bleomycin, a chemotherapeutic antibiotic and pro-fibrotic agent, to induce intervertebral disc fibrosis following needle puncture-induced disc degeneration in rats. X-ray radiographs, MRI imaging, and AFM analysis found that the pharmacological induction of fibrosis of the discs by Bleomycin could also maintain intervertebral disc height. *In vitro* cell-based assays showed that Bleomycin was found to induce BMSCs towards a stronger fibroblast phenotype, and for fibroblastic-like cell AF cells it could promote the migration and Collagen deposition via TGFβ-TGFβR1-SMAD2/3 signaling pathway. Moreover, Bleomycin could upregulate the MMP3 and MMP13 to remodel the ECM (Suppl. Figure 2E), which might help the AF cells to migrate. Despite the structural and compositional differences between healthy NP tissue and fibrotic tissue, the ability of the fibrotic tissue in the NP to maintain the intervertebral disc height may help offset pressure on surrounding tissues and restore some degree of biomechanical stability to the degenerative intervertebral discs.

Mechanistically, we showed using both cellular and molecular-based assays that the TGFβ-TGFβR1-SMAD2/3 is at least involved in the transition of AF cells and BMSCs towards a stronger pro-fibrotic phenotype. This was supported by immunofluorescence staining of intervertebral disc sections from our *in vivo* intervertebral disc degeneration model which show elevated expression of TGFβ, FSP1 and type I collagen in the AF. TGFβ is a potent pro-fibrotic cytokine central to the development of tissue fibrosis[41].

TGFβ modulates fibroblast proliferation and migration, and stimulates ECM production and collagen deposition[42] . Binding of TGFβ to its target receptor (TGFβRI/ALK5 or TGFβRII) on target cells recruits and activates the receptor-regulated effector proteins (R-SMADs), particularly SMAD2 and SMAD3 through direct C-terminal phosphorylation of an SSXS motif. The activated (phosphorylated) SMAD2/3 form trimeric complexes with SMAD4 to translocate into the nucleus to initiate the activation or repression of target genes in cooperation with other transcription factors[43, 44]. TGFβ-SMAD2/3 signaling pathway has been shown to play a key role in the fibrotic process and the dysregulation of TGFβ-SMAD2/3 leads to pathological tissue fibrosis of the lung, liver, and kidney[41, 45-48] . Acting through the TGFβ-TGFβR1-SMAD2/3 axis, we found that Bleomycin promoted migration of AF cells and BMSCs, and also upregulated the expression of key ECM genes such as type 1 collagen as well as type 3 collagen, FN1 in AF cells[49-52]. Pharmacological inhibition of TGFβ signaling with LY346947, a TGFβR1 kinase inhibitor, or with TGFβR1 gene silencing, significantly attenuated the Bleomycin-induced cell migration.

Conclusion

Our pilot study has demonstrated the potential of Bleomycin-induced fibrosis in the management of intervertebral disc degeneration. Bleomycin-induced fibrosis not only maintains intervertebral disc height but also improves the stress tolerance of the degenerative disc. Certainly, more detailed investigations are needed to warrant the potential usefulness of Bleomycin therapy for the treatment of intervertebral disc degeneration in clinical practice.

Abbreviations

IVDD: intervertebral disc degeneration;

IVD: intervertebral disc;

NP: nucleus pulposus;

AF: annulus fibrosus;

MSCs: marrow stromal cells;

LDH: lumbar disc herniation;

DLS: degenerative lumbar spondylolisthesis;

MRI: magnetic resonance imaging;

AFM: atomic force microscopy;

ECM: extracellular matrix;

Declarations

Consent for publication

Written informed consent for publication was obtained from all participants.

Availability of data and materials

All data and materials included in this study are available upon request by contact with the corresponding author

Competing interests

The authors have declared that no competing interests exist

Funding

The work was supported by grants from the National Natural Science Foundation of China (81871790, 81572768 and 81972136) and the Shanghai Hospital Development Center Foundation (SHDC12016110 and 16CR3030A).

Authors' contributions

Jie Zhao, Tangjun Zhou and An Qin guided all the studies. Xiao Yang, Zhiqian Chen performed the experiments, organized the data, and drafted the manuscript. Yifan Zhou and Chen Chen performed the statistical analysis. Chen Han and Xunlin Li helped to draft the manuscript. Haijun Tian, Xiaofei Cheng and Kai Zhang participated in its design. All authors read and approved the final manuscript.

Acknowledgement

We thank Professor Di Chen (Department of Orthopedic Surgery, Rush University Medical Center, Chicago, IL, USA) for providing NP and AF cells. The work was supported by grants from the National Natural Science Foundation of China (81871790, 81572768 and 81972136) and the Shanghai Hospital Development Center Foundation (SHDC12016110 and 16CR3030A).

References

1. Frapin L, Clouet J, Delplace V, Fusellier M, Guicheux J, Le Visage C: **Lessons learned from intervertebral disc pathophysiology to guide rational design of sequential delivery systems for therapeutic biological factors**. *Adv Drug Deliv Rev* 2019, **149-150**:49-71.
2. Smith LJ, Nerurkar NL, Choi K-S, Harfe BD, Elliott DM: **Degeneration and regeneration of the intervertebral disc: lessons from development**. *Dis Model Mech* 2011, **4**(1):31-41.
3. Walter BA, Torre OM, Laudier D, Naidich TP, Hecht AC, Iatridis JC: **Form and function of the intervertebral disc in health and disease: a morphological and stain comparison study**. *J Anat* 2015,

227(6):707-716.

4. Coventry MB, Ghormley RK, Kernohan JW: **The intervertebral disc: Its microscopic anatomy and pathology. Part III. Pathological changes in the intervertebral disc**. *J Bone Joint Surg* 1945, **27**:460-474.
5. Urban JPG, Roberts S: **Degeneration of the intervertebral disc**. *Arthritis Res Ther* 2003, **5**(3):120-130.
6. Roughley PJ: **Biology of intervertebral disc aging and degeneration: involvement of the extracellular matrix**. *Spine* 2004, **29**(23):2691-2699.
7. Sakai D, Grad S: **Advancing the cellular and molecular therapy for intervertebral disc disease**. *Adv Drug Deliv Rev* 2015, **84**:159-171.
8. Ding F, Shao Z-w, Xiong L-m: **Cell death in intervertebral disc degeneration**. *Apoptosis* 2013, **18**(7):777-785.
9. Urban JPG, Smith S, Fairbank JCT: **Nutrition of the intervertebral disc**. *Spine* 2004, **29**(23):2700-2709.
10. Wilkens P, Scheel IB, Grundnes O, Hellum C, Storheim K: **Effect of glucosamine on pain-related disability in patients with chronic low back pain and degenerative lumbar osteoarthritis: a randomized controlled trial**. *JAMA* 2010, **304**(1):45-52.
11. Raj PP: **Intervertebral disc: anatomy-physiology-pathophysiology-treatment**. *Pain Pract* 2008, **8**(1):18-44.
12. Buchowski JM, Adogwa O: **What's New in Spine Surgery**. *J Bone Joint Surg Am* 2019, **101**(12):1043-1049.
13. Sun Y, Zhao Y-b, Pan S-f, Zhou F-f, Chen Z-q, Liu Z-j: **Comparison of adjacent segment degeneration five years after single level cervical fusion and cervical arthroplasty: a retrospective controlled study**. *Chin Med J* 2012, **125**(22):3939-3941.
14. Harrop J, Youssef J, Maltenfort M, Vorwald P, Jabbour P, Bono C, Goldfarb N, Vaccaro A, Hilibrand A: **Lumbar Adjacent Segment Degeneration and Disease After Arthrodesis and Total Disc Arthroplasty**. *Spine* 2008, **33**:1701-1707.
15. Rihn JA, Lawrence J, Gates C, Harris E, Hilibrand AS: **Adjacent segment disease after cervical spine fusion**. *Instr Course Lect* 2009, **58**:747-756.
16. Richardson SM, Hoyland JA, Mobasheri R, Csaki C, Shakibaei M, Mobasheri A: **Mesenchymal stem cells in regenerative medicine: Opportunities and challenges for articular cartilage and intervertebral disc tissue engineering**. *Journal of Cellular Physiology* 2010, **222**(1):23-32.
17. Sakai D: **Stem Cell Regeneration of the Intervertebral Disk**. *Orthopedic Clinics of North America* 2011, **42**(4):555-562.
18. Orozco L, Soler R, Morera C, Alberca M, Sánchez A, García-Sancho J: **Intervertebral disc repair by autologous mesenchymal bone marrow cells: a pilot study**. *Transplantation* 2011, **92**(7):822-828.
19. Tzaan WC, Chen HC: **Investigating the possibility of intervertebral disc regeneration induced by granulocyte colony stimulating factor-stimulated stem cells in rats**. *Adv Orthop* 2011, **2011**.

20. Chen C, Zhou T, Sun X, Han C, Zhang K, Zhao C, Li X, Tian H, Yang X, Zhou Y *et al*: **Autologous fibroblasts induce fibrosis of the nucleus pulposus to maintain the stability of degenerative intervertebral discs**. *Bone Research* 2020, **8**(1):7.
21. Jin Y, Zou Y, Hua C, Chen H, Yang X, Ma G, Chang L, Qiu Y, Lyu D, Wang T *et al*: **Treatment of Early-stage Extracranial Arteriovenous Malformations with Intralesional Interstitial Bleomycin Injection: A Pilot Study**. *Radiology* 2018, **287**(1):194-204.
22. Yang X, Jin Y, Lin X, Chen H, Ma G, Hu X, Qiu Y, Yu W, Chang L, Wang T: **Management of periorbital microcystic lymphatic malformation with blepharoptosis: Surgical treatment combined with intralesional bleomycin injection**. *J Pediatr Surg* 2015, **50**(8):1393-1397.
23. Oh C-d, Im H-J, Suh J, Chee A, An H, Chen D: **Rho-Associated Kinase Inhibitor Immortalizes Rat Nucleus Pulposus and Annulus Fibrosus Cells: Establishment of Intervertebral Disc Cell Lines With Novel Approaches**. *Spine* 2016, **41**(5):E255-E261.
24. Sun L, Mao M, Yan Z, Zuo C, Zhang X: **A Chinese Traditional Therapy for Bleomycin-Induced Pulmonary Fibrosis in Mice**. *Can Respir J* 2018, **2018**:8491487.
25. Olive PL, Banáth JP: **The comet assay: a method to measure DNA damage in individual cells**. *Nat Protoc* 2006, **1**(1):23-29.
26. Degryse AL, Tanjore H, Xu XC, Polosukhin VV, Jones BR, Boomershine CS, Ortiz C, Sherrill TP, McMahon FB, Gleaves LA *et al*: **TGFβ signaling in lung epithelium regulates bleomycin-induced alveolar injury and fibroblast recruitment**. *Am J Physiol Lung Cell Mol Physiol* 2011, **300**(6):L887-L897.
27. Vogt J, Traynor R, Sapkota GP: **The specificities of small molecule inhibitors of the TGFß and BMP pathways**. *Cell Signal* 2011, **23**(11):1831-1842.
28. Cheng F, Shen Y, Mohanasundaram P, Lindström M, Ivaska J, Ny T, Eriksson JE: **Vimentin coordinates fibroblast proliferation and keratinocyte differentiation in wound healing via TGF-β-Slug signaling**. *Proc Natl Acad Sci USA* 2016, **113**(30):E4320-E4327.
29. Vergroesen P-PA, Emanuel KS, Peeters M, Kingma I, Smit TH: **Are axial intervertebral disc biomechanics determined by osmosis?***J Biomech* 2018, **70**:4-9.
30. Qian Y, Qin A, Zheng MH: **Transforaminal ligament may play a role in lumbar nerve root compression of foraminal stenosis**. *Med Hypotheses* 2011, **77**(6):1148-1149.
31. Kitab SA, Miele VJ, Lavelle WF, Benzel EC: **Pathoanatomic basis for stretch-induced lumbar nerve root injury with a review of the literature**. *Neurosurgery* 2009, **65**(1).
32. Zhou X, Wang J, Huang X, Fang W, Tao Y, Zhao T, Liang C, Hua J, Chen Q, Li F: **Injectable decellularized nucleus pulposus-based cell delivery system for differentiation of adipose-derived stem cells and nucleus pulposus regeneration**. *Acta Biomater* 2018, **81**:115-128.
33. Growney Kalaf EA, Pendyala M, Bledsoe JG, Sell SA: **Characterization and restoration of degenerated IVD function with an injectable, in situ gelling alginate hydrogel: An in vitro and ex vivo study**. *J Mech Behav Biomed Mater* 2017, **72**:229-240.

34. Blanco JF, Graciani IF, Sanchez-Guijo FM, Muntión S, Hernandez-Campo P, Santamaria C, Carrancio S, Barbado MV, Cruz G, Gutierrez-Cosío S *et al*: **Isolation and characterization of mesenchymal stromal cells from human degenerated nucleus pulposus: Comparison with bone marrow mesenchymal stromal cells from the same subjects**. *Spine* 2010, **35**(26):2259-2265.
35. Liu LT, Huang B, Li CQ, Zhuang Y, Wang J, Zhou Y: **Characteristics of stem cells derived from the degenerated human intervertebral disc cartilage endplate**. *PLoS ONE* 2011, **6**(10):e26285.
36. Henriksson HB, Svala E, Skioldebrand E, Lindahl A, Brisby H: **Support of concept that migrating progenitor cells from stem cell niches contribute to normal regeneration of the adult mammal intervertebral disc: A descriptive study in the New Zealand white rabbit**. *Spine* 2012, **37**(9):722-732.
37. Henriksson H, Thornemo M, Karlsson C, Hagg O, Junevik K, Lindahl A, Brisby H: **Identification of cell proliferation zones, progenitor cells and a potential stem cell niche in the intervertebral disc region: a study in four species**. *Spine (Phila Pa 1976)* 2009, **34**(21):2278-2287.
38. Liu J, Wang Y, Song L, Zeng L, Yi W, Liu T, Chen H, Wang M, Ju Z, Cong Y-S: **A critical role of DDRGK1 in endoplasmic reticulum homoeostasis via regulation of IRE1α stability**. *Nature Communications* 2017, **8**(1):14186.
39. Chee A, Shi P, Cha T, Kao T-H, Yang S-H, Zhu J, Chen D, Zhang Y, An HS: **Cell Therapy with Human Dermal Fibroblasts Enhances Intervertebral Disk Repair and Decreases Inflammation in the Rabbit Model**. *Global Spine J* 2016, **6**(8):771-779.
40. Shi P, Chee A, Liu W, Chou P-H, Zhu J, An HS: **Therapeutic effects of cell therapy with neonatal human dermal fibroblasts and rabbit dermal fibroblasts on disc degeneration and inflammation**. *Spine J* 2019, **19**(1):171-181.
41. Walton KL, Johnson KE, Harrison CA: **Targeting TGF-β Mediated SMAD Signaling for the Prevention of Fibrosis**. *Front Pharmacol* 2017, **8**:461.
42. Coker RK, Laurent GJ, Shahzeidi S, Lympany PA, du Bois RM, Jeffery PK, McAnulty RJ: **Transforming growth factors-beta 1, -beta 2, and -beta 3 stimulate fibroblast procollagen production in vitro but are differentially expressed during bleomycin-induced lung fibrosis**. *Am J Pathol* 1997, **150**(3):981-991.
43. Shi Y, Massagué J: **Mechanisms of TGF-beta signaling from cell membrane to the nucleus**. *Cell* 2003, **113**(6):685-700.
44. Feng X-H, Derynck R: **Specificity and versatility in tgf-beta signaling through Smads**. *Annu Rev Cell Dev Biol* 2005, **21**:659-693.
45. Chen L, Yang T, Lu D-W, Zhao H, Feng Y-L, Chen H, Chen D-Q, Vaziri ND, Zhao Y-Y: **Central role of dysregulation of TGF-β/Smad in CKD progression and potential targets of its treatment**. *Biomed Pharmacother* 2018, **101**:670-681.
46. Eser PÖ, Jänne PA: **TGFβ pathway inhibition in the treatment of non-small cell lung cancer**. *Pharmacol Ther* 2018, **184**:112-130.
47. Loboda A, Sobczak M, Jozkowicz A, Dulak J: **TGF-β1/Smads and miR-21 in Renal Fibrosis and Inflammation**. *Mediators Inflamm* 2016, **2016**:8319283.

48. Higgins SP, Tang Y, Higgins CE, Mian B, Zhang W, Czekay R-P, Samarakoon R, Conti DJ, Higgins PJ: **TGF-β1/p53 signaling in renal fibrogenesis**. *Cell Signal* 2018, **43**.
49. Verrecchia F, Chu ML, Mauviel A: **Identification of novel TGF-beta /Smad gene targets in dermal fibroblasts using a combined cDNA microarray/promoter transactivation approach**. *J Biol Chem* 2001, **276**(20):17058-17062.
50. Schönherr E, Järveläinen HT, Sandell LJ, Wight TN: **Effects of platelet-derived growth factor and transforming growth factor-beta 1 on the synthesis of a large versican-like chondroitin sulfate proteoglycan by arterial smooth muscle cells**. *J Biol Chem* 1991, **266**(26):17640-17647.
51. Yuan W, Varga J: **Transforming growth factor-beta repression of matrix metalloproteinase-1 in dermal fibroblasts involves Smad3**. *J Biol Chem* 2001, **276**(42):38502-38510.
52. Giannandrea M, Parks WC: **Diverse functions of matrix metalloproteinases during fibrosis**. *Dis Model Mech* 2014, **7**(2):193-203.

Tables

Table 1: patient information

Name	*Pfirrmann Grade*	*Gender*	*Age*	*Diagnosis*
Z	3	male	49	LDH
G	4	male	51	LDH
S	5	female	62	DLS
T	3	male	56	LDH
T	5	male	62	LDH
Zh	4	female	53	LDH
L	4	female	65	DLS
W	3	male	30	LDH
L	5	male	74	LDH
Y	5	femake	39	LDH
M	4	male	57	LDH
Ya	3	female	36	LDH

Table 2: PCR primers information

Gene	Accession Number	Description	5’-Primer-3’
Fn1	NM_019143.2	F	GGATCCCCTCCCAGAGAAGT
		R	GGGTGTGGAAGGGTAACCAG
Col1a1	NM_053304.1	F	GGATCGACCCTAACCAAGGC
		R	GATCGGAACCTTCGCTTCCA
Col3a1	NM_032085.1	F	AGTGGCCATAATGGGGAACG
		R	CACCTTTGTCACCTCGTGGA
TGFβR1	NM_012775.2	F	TGCCTGCTTCTCATCGTGTT
		R	TGCTTTTCTGTAGTTGGGAGT
TGFβR2	NM_031132.3	F	CCAAGTCGGTTAACAGCGAT
		R	TGAAGCCGTGGTAGGTGAAC
TGFβR3	NM_017256.1	F	GAGGGGCTGTCACTTACCAC
		R	CTAATCCCCTCGCTGACCAC
TGFβ1	NM_021578.2	F	CACTCCCGTGGCTTCTAGTG
		R	GGACTGGCGAGCCTTAGTTT

Figures

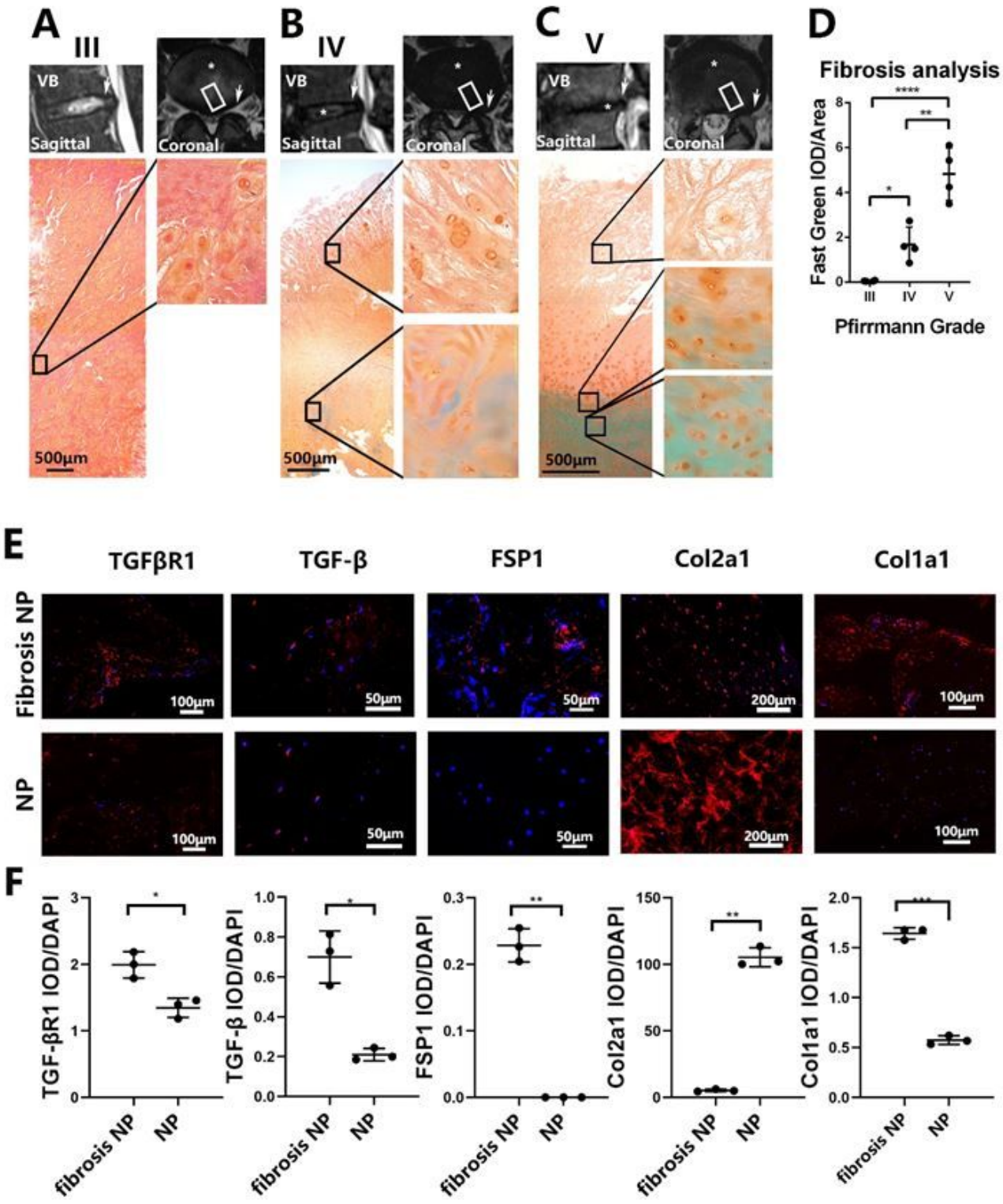

Figure 1

Human intervertebral disc undergone fibrosis with degeneration (a, b, c) Intervertebral disc samples were gathered and their paraffin section were made to undergo Safranin O-Fast Green stain. *Nucleus pulposus region of disc, →Approach to dissect the discs, □Area of samples to be stained (d) IOD level of the green region were analyzed by IPP.6.0 and subsequently calculated with Graphpad8.0 by ordinary one-way ANOVA test. (e) Immunofluorescence assay of TGFβ, TGFβR1, FSP1, Col2a1 and Col1a1 in the

NP region and fibrosis NP region described in a, b, c. (f) IOD level of the red region were analyzed by IPP.6.0 and subsequently calculated with Graphpad8.0 by Student-t test. All data are presented as mean ±sd. from three experiments. *P□0.05, **P□0.01□ ***P□0.001 and ****P□0.0001

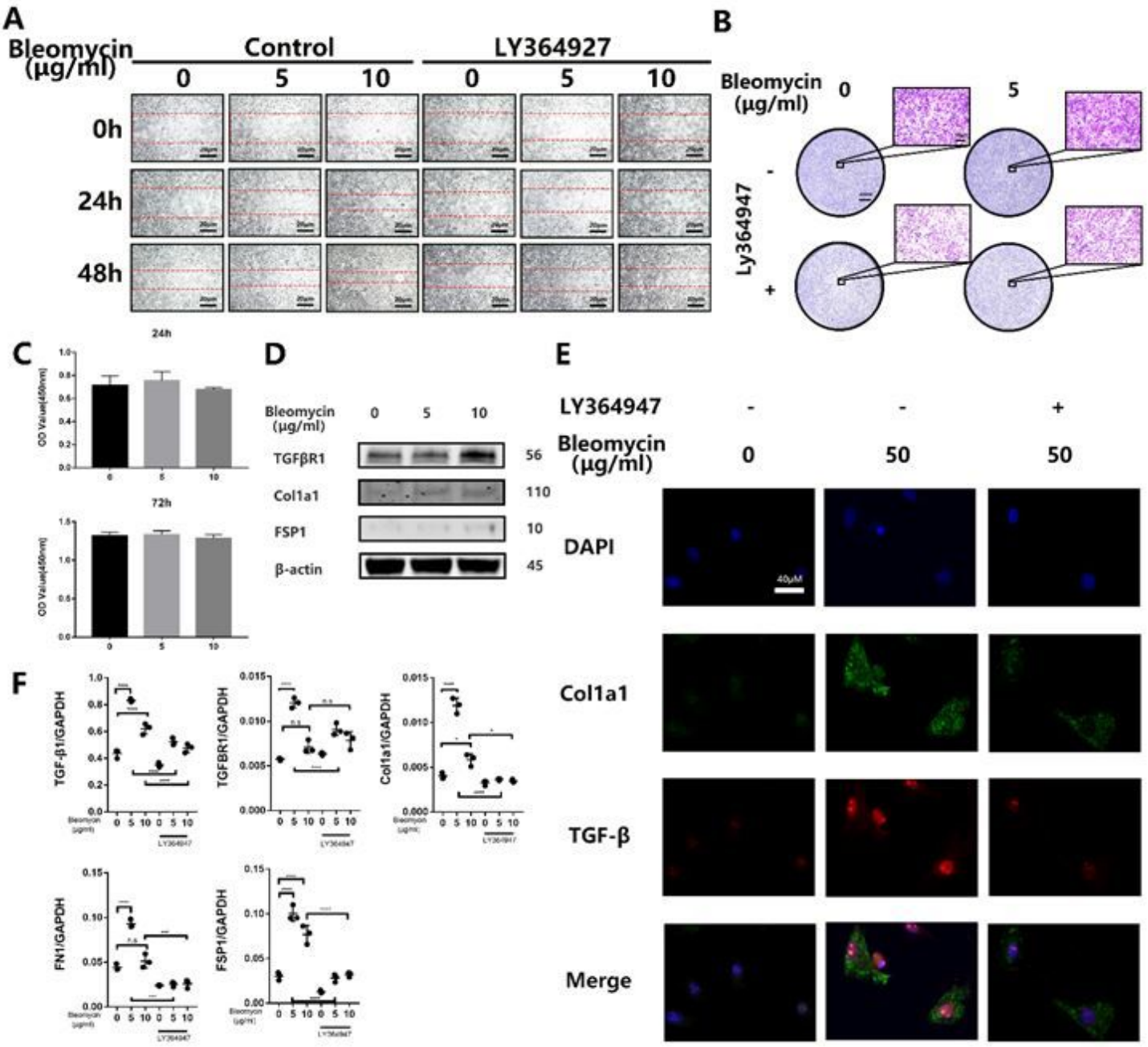

Figure 2

BMSCs was induced to acquire fibrotic phenotype by Bleomycin in vitro. (a, b) BMSC were pretreated with TGFβR1 inhibitor LY364947(10μM) or DMSO and stimulated with Bleomycin in a concentration of 0, 5, 10μg/ml, then cells were cultured for 48 hours and observed in check point of 0, 24 hours and 48 hours to calculate migration rate by wound healing assay or cultured for 24 hours to do transwell test. (c) BMSCs were stimulated with Bleomycin in different concentration of 0, 5, 10μg/ml in 24 and 48 hours, following with cell viability analysis using Cell Count Kit-8 and then subsequently calculated with Graphpad8.0 by

ordinary one-way ANOVA test. (d) Western blot analysis of TGFβR1,FSP1, Col1a1 in BMSCs use β-actin as reference. (e)Immunofluorescence assay of TGFβ and Col1a1 in the BMSCs. (f) Q-PCR analysis of the relative mRNA expression levels of TGFβ, TGFβR1, Fn1, FSP1 and Col1a1 in BMSCs with Bleomycin. All data are presented as mean ±sd. from three experiments. *P<0.05, **P<0.01, ***P<0.001 and ****P<0.0001

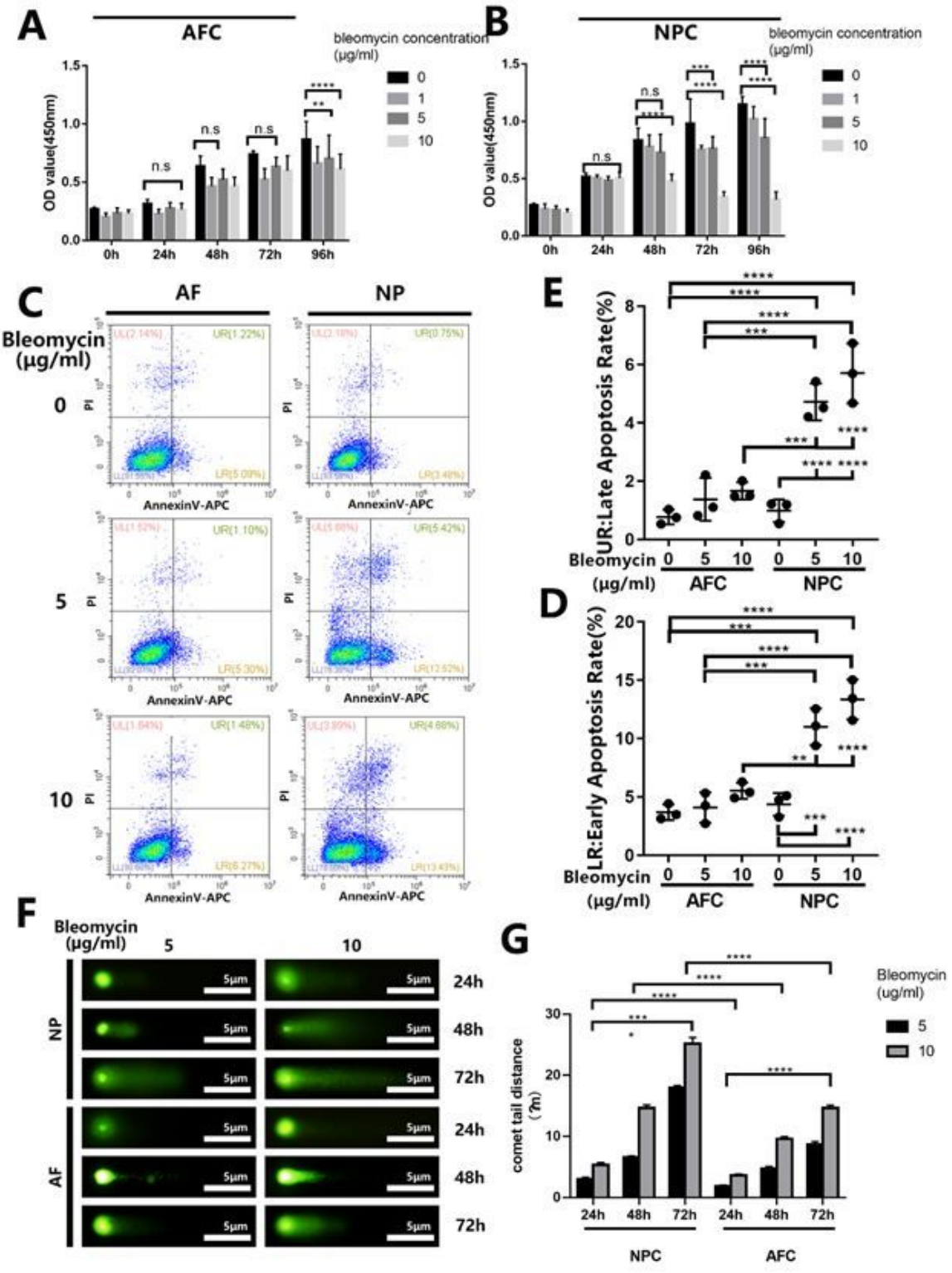

Figure 3

Bleomycin shows little cytotoxicity in AF cells in vitro. (a, b) Cell Count Kit-8 test of AF cells and NP cells were stimulated with Bleomycin in different concentration of 0, 1, 5, 10μg/ml and different time period ranged from 0 to 96 hours. (c) AF cells and NP cells were treated with Bleomycin in a concentration of 0, 5, 10μg/ml and stained with Annexin V and PI, then subjected to flow cytometric analysis. (d, e) Quantification of early and late apoptotic cells rate using Graphpad8.0 by ordinary one-way ANOVA test. (f) AF cells and NP cells were treated with Bleomycin in a concentration of 5, 10μg/ml then stained with Comet assay kit. (g) The degree of DNA damage was measured by comet tail distance using Graphpad8.0 by ordinary one-way ANOVA test. All data are presented as mean ±sd. from three experiments. *P□0.05, **P□0.01□ ***P□0.001 and ****P□0.0001

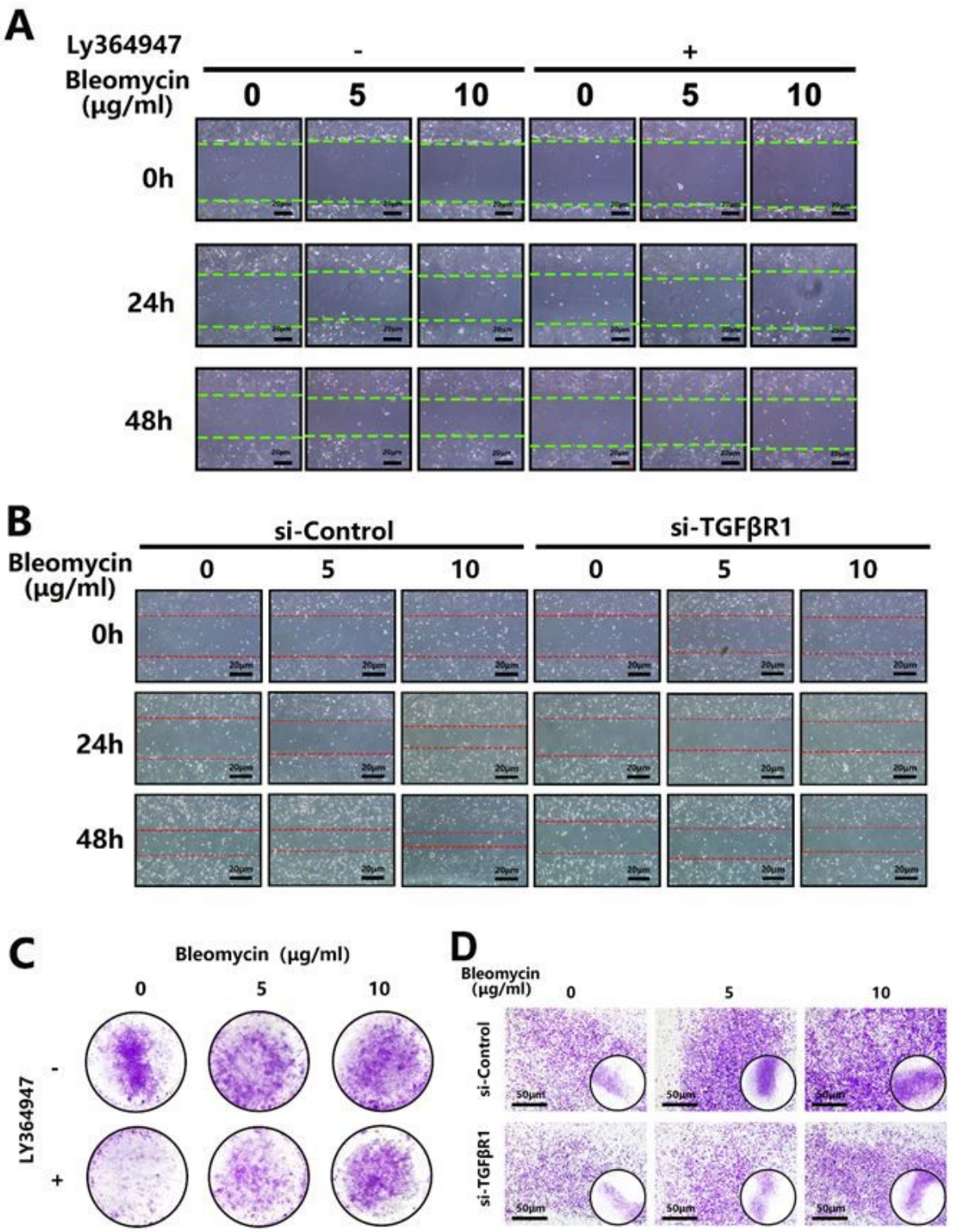

Figure 4

Bleomycin promotes anulus fibrosus cells' migration in vitro. a,c) AF cells were pretreated with TGFβR1 inhibitor LY364947(10μM) or DMSO and stimulated with Bleomycin in a concentration of 0, 5, 10μg/ml, then cells were cultured for 48 hours and observed in check point of 0, 24 hours and 48 hours to calculate migration rate by wound healing assay or cultured for 24 hours to do transwell test. (b,d) Normal and TGFβR1 knocked-down AF cells were stimulated with Bleomycin in a concentration of 0, 5, 10μg/ml, then

cells were cultured for 48 hours and observed in check point of 0, 24 hours and 48 hours to calculate migration rate by wound healing assay or cultured for 24 hours to do transwell test.

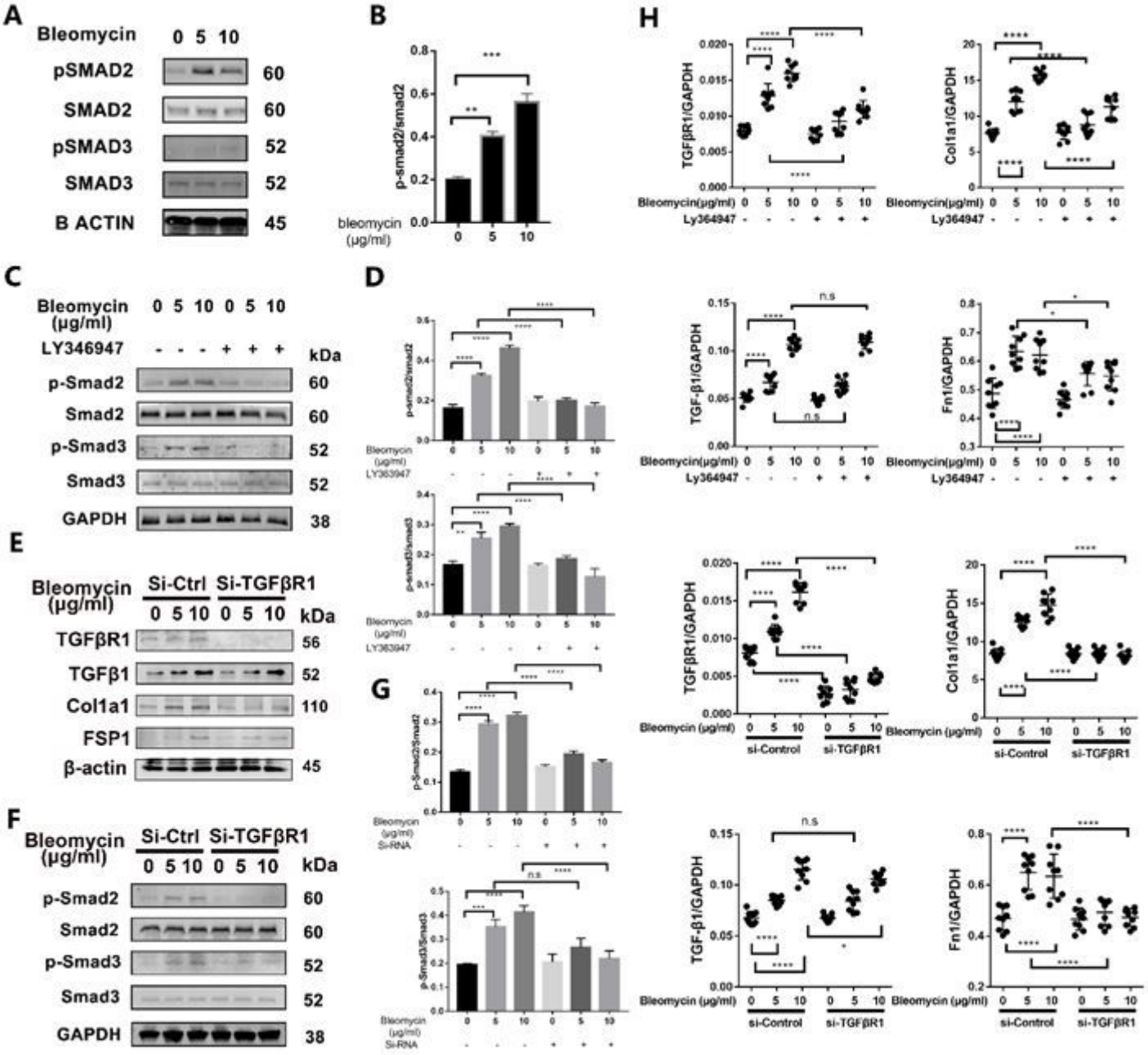

Figure 5

Bleomycin activated the TGF-beta signaling pathway in AF cells. (a,b,c,d) Western blot analysis of phospho-Smad2, phospho-Smad3, Smad2 and Smad3 in AF cells with Bleomycin of 0, 5 and 10μg/ml pretreated with LY346947 or not and Quantification of grey scale value. (e) Western blot analysis of TGFβ, TGFβR1,FSP1, Col1a1 in AF cells use β-actin as reference. (f,g) Western blot analysis of phospho-Smad2, phospho-Smad3, Smad2 and Smad3 in AF cells with or without TGFβR1 knocked-down stimulated by Bleomycin and Quantification of grey scale value. (h) Q-PCR analysis of the relative mRNA expression levels of TGFβ, TGFβR1, Fn1, and Col1a1 in AF cells with Bleomycin or/and LY364947, with or without TGFβR1 knocked-down stimulated by Bleomycin. All qPCR data are calculated with Graphpad8.0

by ordinary one-way ANOVA test and presented as mean ±sd. from three experiments. *P□0.05, **P□0.01□ ***P□0.001 and ****P□0.0001.

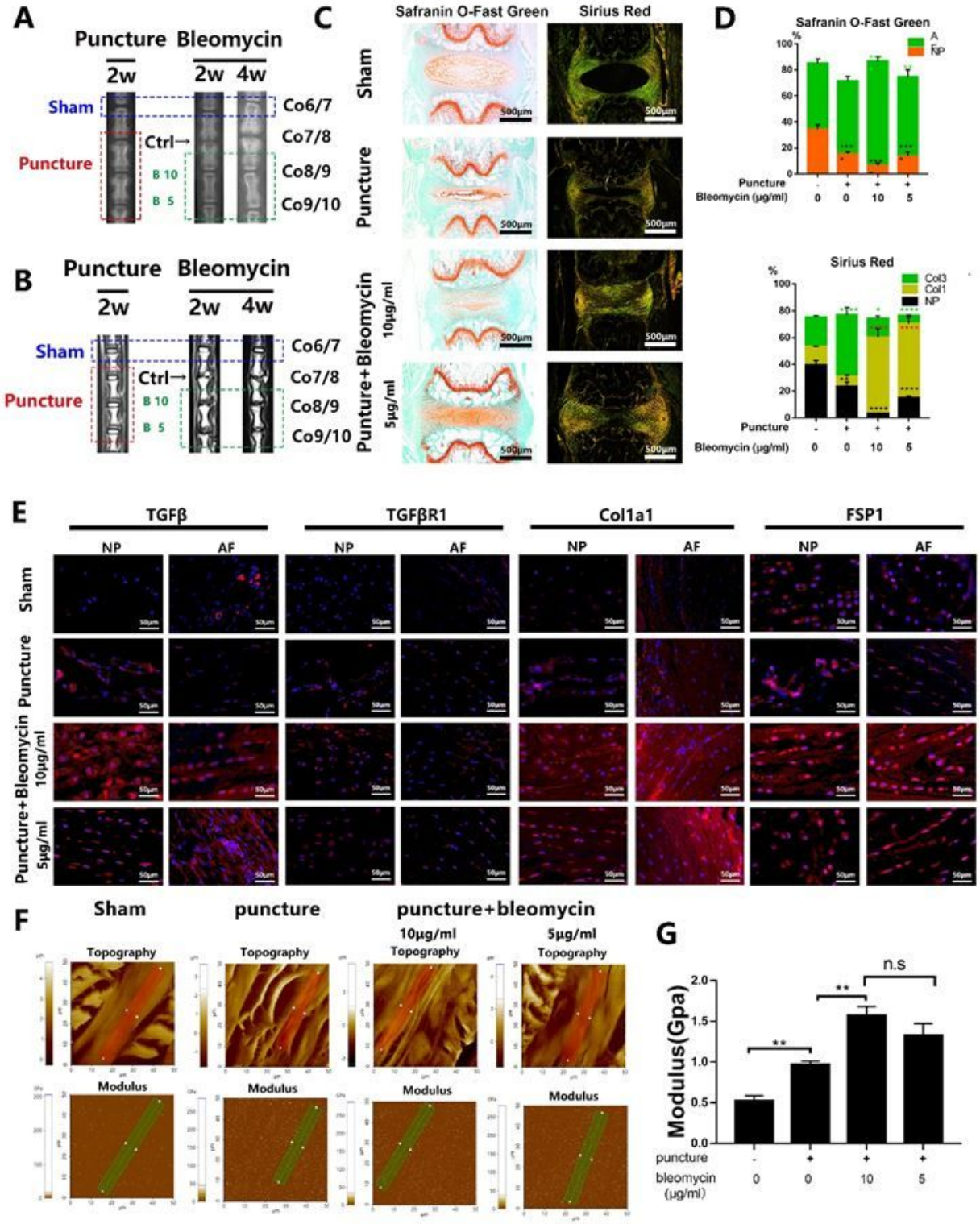

Figure 6

Bleomycin induces degenerated discs fibrosis without height loss in rats. All rats were punctured at Co7/8, Co8/9 and Co9/10, then after two weeks Co8/9 and Co9/10 were rescued by Bleomycin in a concentration of 5, 10μg/ml.(a) X-ray tests of rats at a prone posture and then the pictures were cropped

focused on the area of operation. (b) MRI tests of rats at a supine posture and the T2 signal pictures were chosen. (c) Tails of operation (Co6/7, Co7/8, Co8/9 and Co9/10) were dissected and used to make paraffin section with subsequent Safranin O-Fast Green stain and Sirius Red stain. (d) Proportion quantification of area represent AF region, fibrosis NP region in Safranin O-Fast Green stain, Col1a1, Col3a1 and fibrosis NP region in Sirius Red stain using IPP6.0 and calculated by Graphpad8.0 with ordinary one-way ANOVA test. (e) Immunofluorescence assay of TGFβ, TGFβR1, FSP1 and Col1a1 in the fibrosis NP region and AF region described in c. (f, g) Atomic Force Microscopic of fibrosis AF region in the paraffin section and Quantification of Young's Modulus using XEI of Park System. All data are presented as mean ±sd. from three experiments. *P□0.05, **P□0.01□ ***P□0.001 and ****P□0.0001All data are presented as mean ±sd. from three experiments. *P□0.05, **P□0.01□ ***P□0.001 and ****P□0.0001

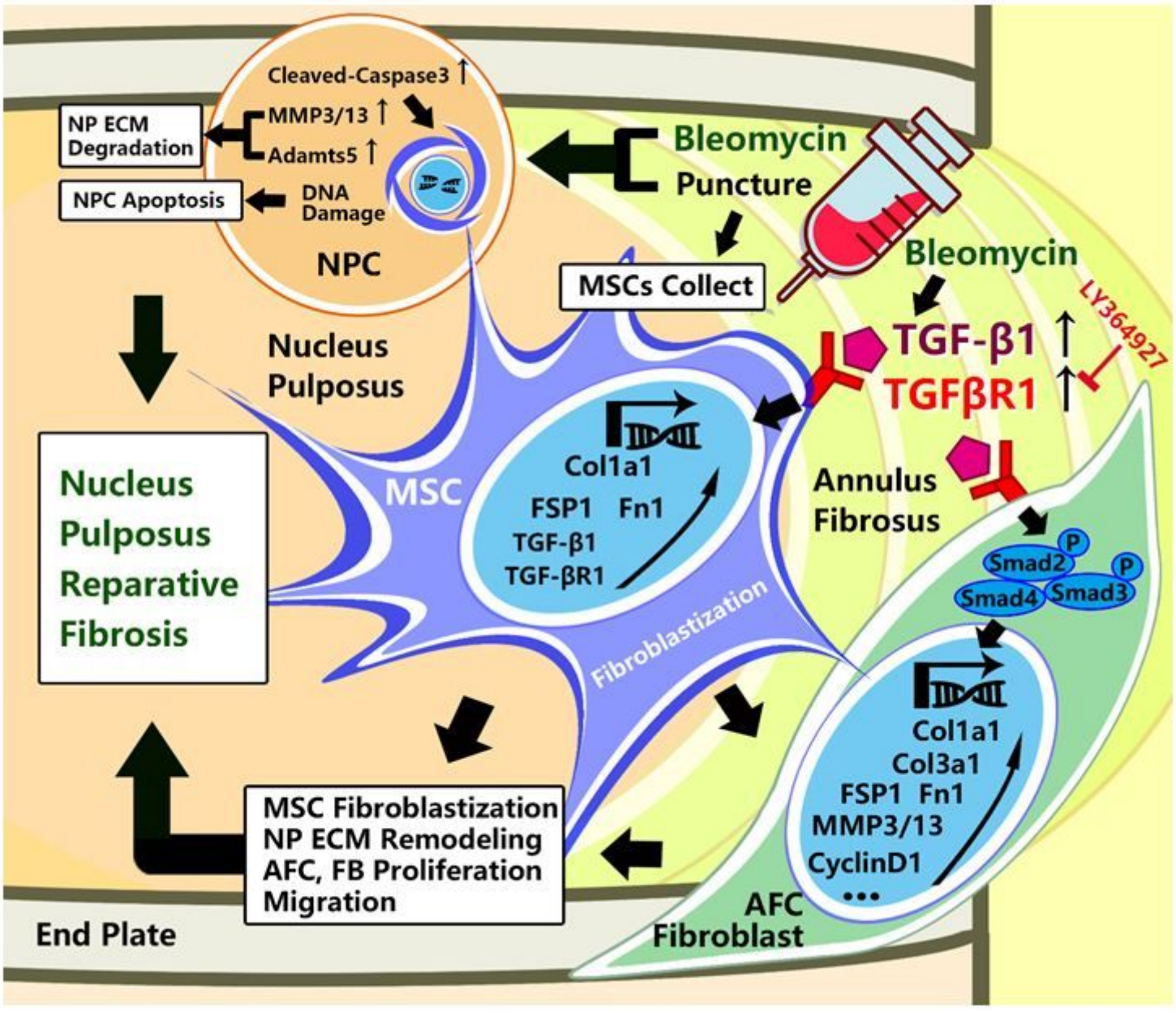

Figure 7

Regulatory function of Bleomycin in fibroblastization of BMSCs in the microenvironment of Nucleus pulposus. Bleomycin could induce fibroblastization of BMSCs, it promotes the fibroblastic transformation of AF cells by increasing the expression of TGFβ, TGFβR1 which activating the TGFβ/Smad2,3 signaling pathway, finally increase the proliferation and migration of these cells. on the other hand, it could stimulate the NP cells to secrete MMP3 and MMP13 to remodel the ECM in the NP that is beneficial for the migration of fibroblastic cells. Locally injection of Bleomycin would increase the Col1a1 and Col3a1 then finally lead to accelerated reparative fibrosis.